DISCRETE AND CONTINUOUS
DYNAMICAL SYSTEMS-SERIES B
Supplement Volume, 2003 pp. 554-562

PHASE-LOCKING IN ELECTRICALLY COUPLED NON-LEAKY INTEGRATE-AND-FIRE NEURONS

Timothy J Lewis

Center for Neural Science and Courant Institute of Mathematical Sciences
New York University
4 Washington Place, Rm 809
New York, NY 10003, USA

Abstract. The synchronization properties of a pair of oscillating spiking neurons connected by electrical (diffusive) coupling is considered. The intrinsic behavior of the cells is described by the non-leaky integrate-and-fire model with a simple modification to account for the effect of spikes. Dynamics of the two-cell system are reduced to the consideration of a one-dimensional map. Periodic orbits of the map correspond to phase-locked solutions of the paired-cell system. The bifurcation structure of the map and therefore the phase-locked states in the two-cell system are analyzed. It is shown that increasing the effect of the spikes and increasing the intrinsic frequency of the cells promote synchronous activity. However, in some conditions, increasing the strength of electrical coupling can counter-intuitively lead to the destabilization of synchronous activity and the stabilization of the anti-phase state.

1. **Introduction.** Recently, it has been found that many inhibitory neurons in the brain are linked by direct electrical coupling [2, 4]. We are only beginning to understand how the intrinsic spiking activity of these neurons and the electrical coupling give rise to the behavior in inhibitory cell networks. Theoretical studies have examined the phase-locking of electrically coupled pairs of leaky integrate-and-fire (IF) cells in the weak coupling limit [6] and of electrically coupled cells described by the spike response model [3]. In the same vein as this previous work, we examine the phase-locking structure of two electrically coupled non-leaky IF cells. The simplicity of the non-leaky IF model allows a thorough analytical characterization of how solutions depend on the parameters governing the intrinsic cellular dynamics and the strength of the coupling. Despite its simplicity, however, the non-leaky IF system captures the qualitative features of the leaky IF system.

2. **Electrically coupled non-leaky IF cells.** Two identical cells connected by electrical coupling are considered. The intrinsic dynamics of individual cells are described by single-compartment non-leaky IF dynamics.

$$\begin{cases} C\dfrac{dV_1}{d\tilde{t}} = I + \ g_c\ (V_2 - V_1) \\ C\dfrac{dV_2}{d\tilde{t}} = I + \ g_c\ (V_1 - V_2), \end{cases} \tag{1}$$

where $\tilde{t}$ is time, V_j is the transmembrane potential of the j^{th} cell ($j = 1, 2$), I is a constant current applied to the cells, C is the capacitance of the cell membrane, and

1991 *Mathematics Subject Classification.* Primary: 92C20, 92C30; Secondary: 34A47.
Key words and phrases. Electrical Coupling, Phase-locking, Integrate-and-fire.

g_c is the electrical coupling conductance. When V_j reaches a threshold potential V_{th}, cell j "fires a spike" and V_j is reset to the potential V_r. We will assume that I is a positive, constant parameter. Thus, the cells intrinsically oscillate with a period $(V_{th}-V_r)I/C$. Electrical coupling is modeled as a constant ohmic resistance (diffusive coupling) with current flowing down the potential gradient. (The leaky IF model includes an additional "leakage" term, $-g_m V_j$, on the right-hand side of the differential equation for V_j).

When a neuron's membrane potential exceeds its threshold potential, there is a large, but short-lived, increase in the membrane potential before the potential falls to a subthreshold value. We will refer to this transient suprathreshold excursion as the "spike". Integrate-and-fire models usually do not include the effects of spikes, i.e. once the transmembrane potential reaches threshold, it is reset to V_r. However, the effect of spikes can be important in determining phase-locking patterns [3, 6], and therefore it must be included in any adequate model of electrically coupled cells. Here, we approximate tall, thin spikes by modeling the spike as a delta-function with area $\tilde{\beta}$ [6]. Thus, when a spike is elicited in one cell, the potential of the other cell instantaneously increases by a fixed amount, $g_c\tilde{\beta}/C$.

Setting $g = g_c\ (V_{th}-V_r)/I$, $v_j = (V_j - V_r)/(V_{th}-V_r)$, $\beta = \tilde{\beta}I/(C(V_{th}-V_r)^2)$ and $t = \tilde{t}I/(C(V_{th}-V_r))$, we change to non-dimensional variables. All dimensional parameters are contained in just two parameters, g and β. The governing equations in non-dimensional form are

$$\begin{cases} \dfrac{dv_1}{dt} = 1 + \ g\ (v_2 - v_1) \\ \dfrac{dv_2}{dt} = 1 + \ g\ (v_1 - v_2) \end{cases} \tag{2}$$

The non-dimensional threshold and reset potentials are 1 and 0 respectively, and the period of the intrinsic oscillations is 1. When a cell fires a spike, the membrane potential of the other cell is knocked towards threshold by an amount $g\beta$.

3. **Reduction to a one-dimensional map.** Without loss of generality, we take the initial conditions of cell 1 to be at the reset potential and cell 2 to be at some arbitrary potential, $v_1(0) = 0$, $v_2(0) = u_0 \in [0,1]$. The subthreshold behavior of the two-cell system can be found by solving equations 2,

$$\begin{cases} v_1(t) = t + \dfrac{u_0}{2}(1 - e^{-2gt}) \\ v_2(t) = t + \dfrac{u_0}{2}(1 + e^{-2gt}). \end{cases} \tag{3}$$

From inspection of equations 3, it is easy to see that during subthreshold activity the cells maintain the order of their membrane potentials, $0 \le v_1(t) \le v_2(t) \le 1$. This guarantees that cell 2 will reach threshold before cell 1 (if $u_0 \neq 0$). When cell 2 fires and is reset, either (i) the cells immediately synchronize (the firing of cell 2 knocks cell 1 above threshold) or (ii) the order of the membrane potentials is reversed and cell 1 will be the next cell to fire. This ordering principle implies that only 1:1 phase-locked rhythms are possible.

Below, we will first find the time that it takes cell 2 to reach threshold and fire (t_f) as a function of its initial condition u_0. We will then find the membrane potential of cell 1 after cell 2 fires (u_1) as a function of u_0. This will allow us to define a one-dimensional map that completely captures the dynamics of the two-cell system.

The time that it takes cell 2 to reach threshold and fire is given by $v_2(t_f) = 1$,

$$t_f + \frac{u_0}{2}(1 + e^{-2gt_f}) = 1. \tag{4}$$

Equation 4 is a transcendental equation for t_f in terms of u_0. However, we can determine the dependence of t_f on u_0 by examining u_0 as a function of t_f,

$$u_0 = U(t_f) = 2\frac{1 - t_f}{1 + e^{-2gt_f}}. \tag{5}$$

We will show that U is invertible in the physically relevant region, $u_0 \in [0, 1]$ and $t_f > 0$.

Because $U(t_f) < 0$ for $t_f > 1$, we immediately restrict the domain of $U(t_f)$ to $t_f \in [0, 1]$. We can restrict the domain of $U(t_f)$ even further in certain cases. One can readily show that $U(0) = 1$, $U(1) = 0$, and $U'(0) = -1 + g$. Furthermore, $U''(t_f) < 0$ for $t_f \in [0, 1]$ and $g > 0$. From these facts, we find that, for $g > 1$, $U(t_f) > 1$ for $t_f \in (0, t_{fA})$, where

$$U(t_{fA}) = 2\frac{1 - t_{fA}}{(1 + e^{-2gt_{fA})}} = 1.$$

The equation for t_{fA} is transcendental, but it is easy to show that $0 < t_{fA} < 1/2$ and that t_{fA} monotonically increases with increasing $g > 1$. For $0 < g \leq 1$, $U(t_f) \leq 1$ for $t_f \in [0, 1]$. By extending our definition of t_{fA} so that $t_{fA} = 0$ for $0 < g \leq 1$, the physically relevant domain of $U(t_f)$ can be concisely written as $\Omega = \{0 \cup (t_{fA}, 1]\}$. When restricted to the domain Ω, U is invertible

$$t_f = U^{-1}(u_0) = T_f(u_0).$$

The implicitly defined function $T_f(u_0)$ gives the time that it takes cell 2 to fire given that its initial membrane potential is u_0 and cell 1 is initially at the reset potential. $T_f(u_0)$ is continuous on $u_0 \in [0, 1)$. A discontinuity exists at $u_0 = 1$ when $g > 1$,

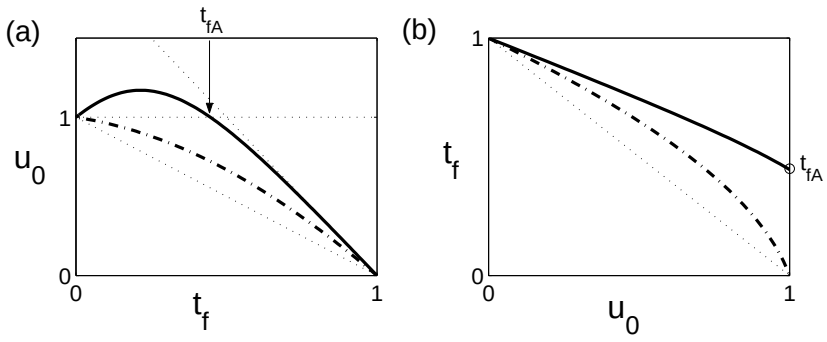

FIGURE 1. $U(t_f)$ and $T_f(u_0)$ for $g = 2.5$ (solid lines) and $g = 0.7$ (dot-dashed lines). t_{fA} is indicated for $g = 2.5$. The thin dotted lines in (a) are (i) $2(1 - t_f)$, the upper bound of $U(t_f)$ $(g \to \infty)$, (ii) $1 - t_f$, the lower bound of $U(t_f)$, $(g = 0)$, and (iii) the constant function 1. The thin dotted line in (b) is $1 - u_0$, the lower bound of $T(u_0)$ $(g = 0)$.

where $\lim_{u\to 1^-} T_f(u) = t_{fA}$ and $T_f(1) = 0$. $T_f(u_0)$ is monotonically decreasing and $T_f''(u_0) \le 0$ for $u_0 \in [0,1]$.

The value of v_1 immediately before the spike in cell 2 as a function of u_0 is obtained by substituting $t = T_f(u_0)$ into equation 3

$$v_1(t_f^-) = T_f(u_0) + \frac{u_0}{2}(1 - e^{-2gT_f(u_0)}) = 2T_f(u_0) - (1 - u_0),$$

where the relationship $e^{-2gT_f(u_0)} = 2(1 - T_f(u_0))/u_0 - 1$ given by equation 4 has been used to simplify the expression for $v_1(t_f^-)$. The potential of cell 1 immediately after the spike in cell 2 ($v_1(t_f^+) = u_1$) is found by adding the spike effect $g\beta$ to $v_1(t_f^-)$. If $v_1(t_f^-) + g\beta > 1$, then the spike in cell 2 knocks the membrane potential of cell 1 above threshold and the cells will immediately synchronize. Therefore, $v_1(t_f^-) + g\beta$ is truncated to ensure that $u_1 \le 1$. We define u_B to be the value of u_0 below which truncation is necessary,

$$2T_f(u_B) - (1 - u_B) + g\beta \equiv 1.$$

The case of $u_0 = 1$ ($v_1(0) = 0, v_2(0) = 1$) implies that cell 1 has just fired and been reset, and it has knocked cell 2 to threshold. The cells immediately synchronize and are reset simultaneously upon the subsequent firing, therefore $u_1 = 0$. In summary, the membrane potential of cell 1 after cell 2 fires and is reset is given by

$$u_1 = \psi(u_0) = \begin{cases} 1 & , \quad 0 \le u_0 < u_B \\ 2T_f(u_0) - (1 - u_0) + g\beta & , \quad u_B \le u_0 < 1 \\ 0 & , \quad u_0 = 1 \end{cases} \tag{6}$$

Because the system is symmetric, we can apply the same argument to get the potential of cell 2 after cell 1 fires. Indeed, equation 6 yields a one-dimensional return map that captures all behavior of the coupled cells,

$$u_{k+1} = \psi(u_k).$$

For odd k, the variable u_k corresponds to the value of v_2 when cell 1 fires; for even k, u_k corresponds to the value of v_1 when cell 2 fires. By iterating the one-dimensional return map, we can observe the dynamics of the coupled cell system. These dynamics depend on the two parameters, the electrical coupling strength g and the strength of the spike effect β.

4. **Analysis of return map.** Figure 2 provides a summary of the existence and stability of the phase-locked solutions in the two-cell system in g-β parameter space.

The phase-locking structure is determined by a few basic properties of the map ψ. Most of these properties are inherited from $T_f(u)$. ψ maps $[0,1]$ into $[0,1]$. ψ is continuous on $[0,1)$ and has a discontinuity at $u = 1$ for $\beta > 0$ and/or $g > 1$, in which case $\psi(1) = 0$ and

$$\lim_{u\to 1^-} \psi(u) \equiv u_A + g\beta = 2t_{fA} + g\beta > 0,$$

i.e. u_A is the size of the jump discontinuity at $u = 1$ with $\beta = 0$. Note that the spike effect $g\beta$ appears to be a simple lift of the map, but there is also the truncation that ensures that $\psi(u) \le 1$. On $[u_B, 1]$, the map is monotonically decreasing and $\psi''(u) < 0$.

$\psi(0) = 1$ and $\psi(1) = 0$ define a period-2 orbit that corresponds to synchronous activity in the coupled cells. This period-2 orbit, which we will refer to as the synchronous solution, always exists. The period of the synchronous activity is given by $T_f(0) + T_f(1) = 1$, i.e. it is equal to the intrinsic period of the cells. When

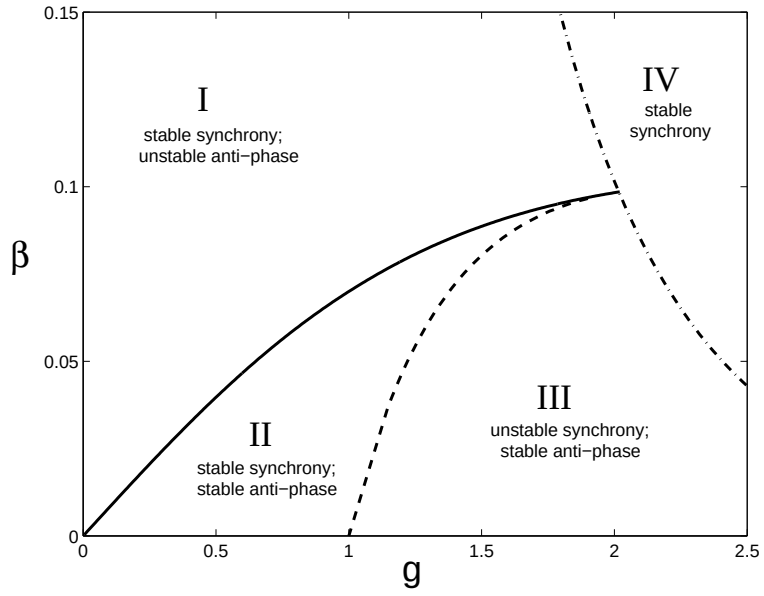

FIGURE 2. Summary of the phase-locking regions for the electrically coupled cell-pair and solutions for the one-dimensional return map in g-β parameter space. Above the dot-dashed line, $u_A + g\beta > 1$ and $\psi(u) = 1$ for $u \in [0, 1)$. Above the dashed line, $u_A + g\beta < u_B$; below the dashed line, $u_A + g\beta > u_B$. The change in stability of the anti-phase solution occurs along the solid line, given by the equality of equation 7, i.e. period doubling bifurcations occur along the solid line. Thus, the lines divide parameter space into four regions with different stability of the synchronous and the anti-phase solutions. Note that for $\beta = 0$, the synchronous solution is not stable (not shown on diagram).

the coupling strength and the spike effect are strong enough to have $u_A + g\beta \geq 1$, $\psi(u) = 1$ for $u \in [0, 1)$ and $\psi(1) = 0$. In this case, the synchronous state is the only phase-locked state that exists, and it is achieved immediately after cell 2 fires. (The transition line $u_A + g\beta = 1$ is plotted as a dot-dashed line in figure 2).

Because ψ is continuous and monotonically decreasing in $(u_B, 1)$ with $\psi(u_B) = 1$, there exists a unique fixed point u^* when $\lim_{u\to 1^-} \psi \equiv u_A + g\beta < 1$, i.e. $u^* = \psi(u^*)$, $u^* \in (u_A + g\beta, 1)$. This unique fixed point corresponds to anti-phase activity in the coupled cells (when one cell fires, the other cell's membrane potential is u^*), and therefore the fixed point will be referred to as the anti-phase solution. The anti-phase solution can be explicitly calculated using $u^* = \psi(u^*)$ and $T_f^{-1}(u^*)$,

$$u^* = T_f^{-1}(\frac{1 - g\beta}{2}) = \frac{1 + g\beta}{1 + e^{-g(1-g\beta)}}, \qquad t_f^* = T_f(u^*) = \frac{1 - g\beta}{2}.$$

u^* and t_f^* decrease with β and g. The period of the anti-phase activity in the two-cell system is $2t_f^* = 1 - g\beta$, which implies that anti-phase activity is always faster than synchronous activity. u^* does not exist when $T_f^{-1}(\frac{1-g\beta}{2}) > 1$, i.e. $u_A + g\beta > 1$.

The synchronous solution is stable if $\psi'(0)\psi'(1) < 1$, i.e. period-2 solutions are stable when $|\psi'(u_1^*)||\psi'(u_2^*)| < 1$, where $\psi(u_1^*) = u_2^*$ and $\psi(u_1^*) = u_2^*$. Let us examine the stability of the synchronous solution in four different conditions. Examples of these cases are depicted in figure 3.
(a) When $\beta = 0$ (no spike effect included) and $0 < g \leq 1$ (ψ continuous),

$$0 \leq \psi'(0)\psi'(1) \;=\; (2T_f'(0)+1)(2T_f'(1)+1) \;=\; e^{-2g}\frac{1+g}{1-g} \;<\; 1.$$

This implies that the synchronous solution is never stable. The divergence away from the synchronous solution is very slow for small positive g, but the rate of divergence increases as g increases and is unbounded as g approaches 1.
(b) When $\beta = 0$ and $g > 1$ (ψ discontinuous at 1), $\psi'(0) < 0$ while $\psi'(1)$ is unbounded. Thus, the synchronous solution is unstable.
(c) $\beta > 0$ and $0 < g \leq 1$. $\psi'(1)$ is unbounded, but $\psi(u) = 1$ for $u \in [0, u_B]$. The synchronous solution is stable to small positive perturbations from 0. Although small negative perturbations from 1 knock the state of the system to $u \sim g\beta$, points around $u \sim g\beta$ are immediately mapped back to 1, i.e. $g\beta \leq u_B$, which follows

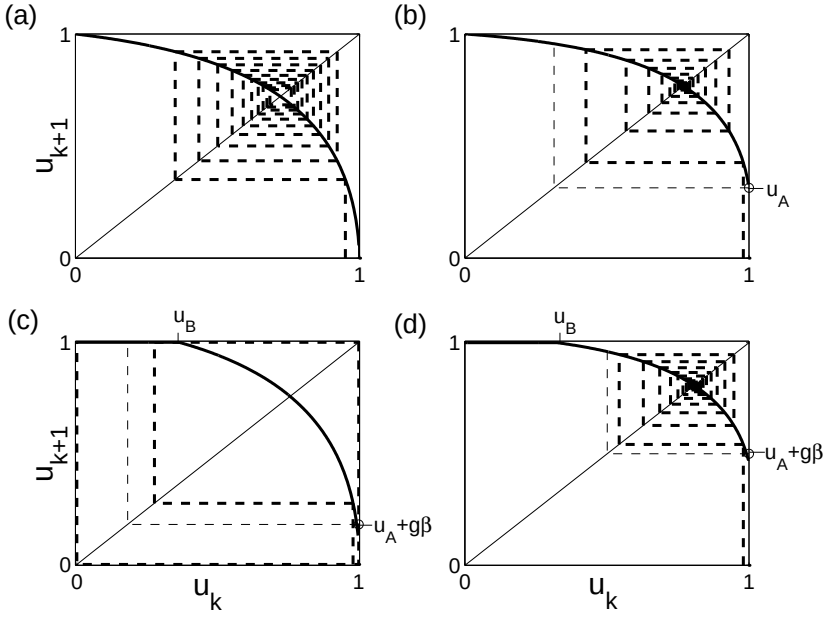

FIGURE 3. Examples of return maps, $u_{k+1} = \psi(u_k)$. The thick solid line is $\psi(u)$; the thick dashed lines show cobweb iterations of the map. The thin dashed line demarks $u_A + g\beta$. In (a) $\beta = 0$, $g = 0.95$ and (b) $\beta = 0$, $g = 1.2$, the synchronous solution ($\psi(0) = 1$, $\psi(1) = 0$) is unstable and the anti-phase solution (the fixed point) is stable. (c) $\beta = 0.1$, $g = 0.9$. The synchronous solution is stable ($u_B > u_A + g\beta$); the anti-phase is also stable for these parameters. (d) $\beta = 0.03$, $g = 1.3$. The synchronous solution is unstable ($u_B < u_A + g\beta$) and the anti-phase is stable.

from $T_f(u) \geq (1-u)$ and $1 \equiv 2T_f(u_B) - (1-u_B) + g\beta$. Thus, the synchronous solution is stable.
(d) $\beta > 0$ and $g > 1$. As in (c), $\psi(u) = 1$ for $u \in [0, u_B]$, so the synchronous solution is stable to small positive perturbations from 0. However, $u_A + g\beta < u_B$ does not always hold, and therefore, small negative perturbations from 1 do not always return to 1. The synchronous solution is stable if and only if $u_A + g\beta < u_B$ or $u_A + g\beta \geq 1$. ($u_A + g\beta = u_B$ is plotted as a dashed line in figure 2).

It is interesting to note that stability of synchronous activity is strictly a result of spike effect. If v_2 is sufficiently small when v_1 is reset to 0, then when v_2 reaches threshold and fires, the spike effect will be strong enough to kick v_1 over threshold and the cells will immediately synchronize.

The anti-phase solution is stable when $|\psi'(u^*)| < 1$,

$$0 > \psi'(u^*) = 2T_f'(u^*) + 1 = \frac{2}{U'(t_f^*)} + 1 > -1.$$

This stability condition can be simplified to

$$sinh(g(1-g\beta)) - g(1+g\beta) > 0. \tag{7}$$

This condition implies that when the spike effect is zero ($\beta = 0$) or when β is small and $g \sim O(1)$, the anti-phase solution is stable, and when g is small and $\beta \gg g$, the anti-phase solution is unstable. However, the stability criterion is relevant only when $g < g^* \sim 2.016$, where g^* is the critical value of g at which $\lim_{u\to 1^-} \psi'(u) = -1$. g^* is found using $\psi'(u \to 1^-) = -1$ and the definition of t_{fA}.

For $g > g^*$, $\psi(u) > -1$ for all $u \in (0,1)$. This implies that, for $g > g^*$, the stability of the anti-phase solution cannot change with changes in β: when the anti-phase solution exists ($u_A + g\beta < 1$), it is stable. For $g < g^*$, there exists a unique $u_{pd} \in (0,1)$ such that $\psi'(u_{pd}) = -1$, $\psi'(u) > -1$ for $u \in (0, u_{pd})$, and $\psi'(u) < -1$ for $u \in (u_{pd}, 1)$. Therefore, when $g < g^*$, the anti-phase solution is guaranteed to change from stable to unstable as β increases from 0. The line of the stability transition points in g, β-parameter space is given by the equality corresponding to condition 7 (shown by the solid line in figure 2). As g increases, the value of β at which the change in stability takes place monotonically increases from $\beta = 0$ for $g = 0$ to $\beta^* = 1/(g^*(2g^* + 1)) \sim 0.0985$ when $g = g^*$. The expression for β^* is found using $u_A + g\beta = 1$.

Figure 4 provides two examples of bifurcation diagrams: one for fixed g and the other for fixed β. The change in stability of the anti-phase solution is associated with a period doubling bifurcation in the map ($\psi'(u^*) = -1$, $\psi''(u^*) < 0$). This bifurcation can be shown to be subcritical, giving rise to an unstable period-2 orbit. The unstable period-2 orbit corresponds to asynchronous, but non-anti-phase, activity in the cells. It is the only other phase-locked state besides the synchronous and anti-phase solutions. The Poincaré-Bendixson Theorem implies that the unstable period-2 solution exists when both the synchronous solution and anti-phase solutions are stable (region II in figure 2). The unstable period-2 orbit separates the basins of attractions of the two stable solutions. The loss of stability of the synchronous solution at $u_B = u_A + g\beta$ is associated with the parameter values at which the asynchronous period-2 orbit goes to $\psi(u_B) = 1$ and $\psi(1) = u_B$. Note that the period-2 orbit cannot exist for $g \geq g^*$, because $\psi(u) > -1$ for all $u \in (0,1)$ in this case.

Also, note that, as $(g, \beta) \to (g^*, \beta^*)$ from below, $u_A + g\beta \to 1$. Therefore, as $(g, \beta) \to (g^*, \beta^*)$ from below, $u_B = u_A + g\beta \to 1$. Thus, the three transition lines

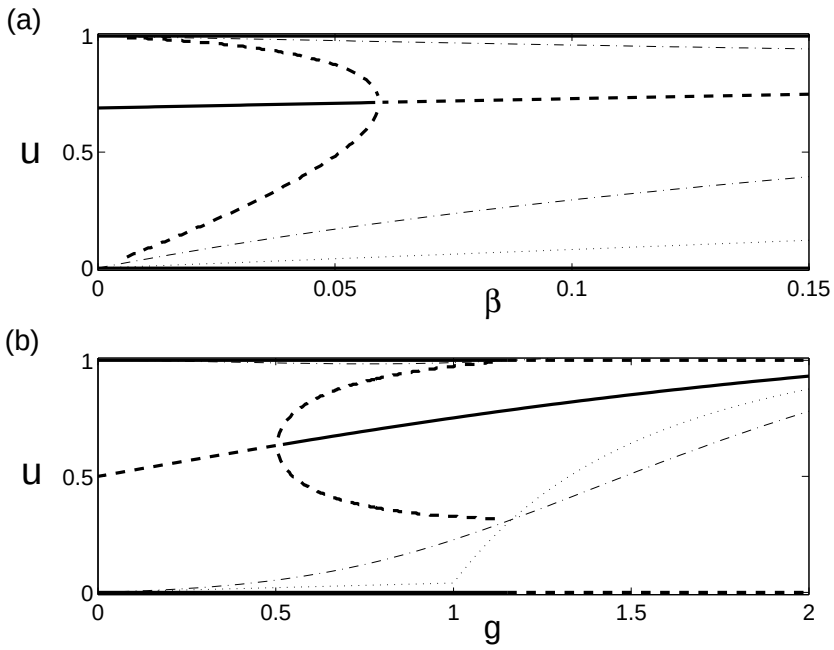

FIGURE 4. Bifurcation diagrams for (a) $g = 0.8$ and (b) $\beta = 0.04$. Thick lines denote periodic orbits of the map (phase-locked states of the two-cell system) including the period-2 orbits. Thick dashed lines and thick solid lines denote unstable and stable states respectively. The thin dot-dashed lines represent u_B and its preimage. The thin dotted line represents $u_A + g\beta$.

in figure 2 meet at one point (g^*, β^*). This is a consequence of the discontinuity of $\psi(u)$ at $u = 1$ and, in general, would not occur if $\psi(u)$ was continuous.

5. **Discussion.** It is not surprising that electrical coupling can lead to synchronous activity, but it can also support asynchronous activity [7, 5, 3, 6]. The exact conditions for promoting synchronous or asynchonous behavior remain unclear, but the work presented here and previous work [3, 6] begin to construct a framework for understanding dynamics in populations of spiking neurons connected by electrical coupling.

Spikes play an essential role in determining phase-locking behavior [3, 6]. When the effect of spikes are neglected, only anti-phase activity is stable in non-leaky IF cells and in weakly coupled leaky IF cells. In both of these models, increasing the strength of the spike effect (i.e. the area under the spike) promotes synchronous activity [6]. It should be pointed out, however, that this is not a general rule. There are many cases where the model we use here is inappropriate. For instance, when spikes are wide or when cells are not electrotonically compact, spikes can promote asynchronous activity [3, 1].

When the dependence of g and β on I is examined with respect to figure 2, we see that decreasing I can lead to stable anti-phase activity (given that $\tilde{\beta} g_c/(C(V_{th} - V_r))$

is sufficiently small). That is, anti-phase activity can occur when the intrinsic frequency of the cells is low, whereas only synchronous activity is stable at high frequencies. This agrees with results for leaky IF model [6]. It is also consistent with the observation that electrical coupling can give rise to anti-phase behavior when the intrinsic dynamics of the cells are close to a homoclinic bifurcation [5].

One would generally assume that increasing electrical coupling strength should promote synchrony. When electrical coupling is sufficiently strong or when the effect of spikes is large, this is indeed the case for non-leaky IF system. However, we have shown that, for sufficiently small β, increasing the electrical coupling strength can destabilize synchronous activity and lead to stable anti-phase activity. The cellular dynamics required for this phenomenon to occur in more complicate models and real neurons have yet to be studied, however a sharp reset in the membrane potential following a spike is likely to be essential.

Acknowledgements The authors would like to thank the anonymous reviewers for their comments on the manuscript. TJL is supported by an National Institute of Mental Health postdoctoral fellowship MH12873.

REFERENCES

[1] V. A. Alvarez, C. C. Chow, E. J. Van Bockstaele and J. T. Williams, *Frequency-dependent synchrony in locus ceruleus: Role of electrotonic coupling*, Proc. Natl. Acad. Sci. USA 99, (2002) 4032–4403.

[2] Y. Amitai, J. R. Gibson, M. Beierlein, S. L. Patrick, A. M. Ho, B. W. Connors and D. Golumb, *Spatial organization of electrically coupled networks of interneurons in neocortex*, J.Neurosci. 22 (2002), 4142–4152.

[3] C. C. Chow and N. Kopell, *Dynamics of spiking neurons with electrical coupling*, Neural Comp. 12 (2000), 1643–1678.

[4] M. Galarreta and S. Hestrin, *Electrical synapses between GABA-releasing interneurons*, Nat. Rev. Neurosci. 2 (2001), 425–433.

[5] S. K. Han, C. Kurrer and Y. Kuramoto *Diffusive interactions leading to dephasing of coupled neural oscillators*, Int. J. Bif. Chaos 7 (1997), 869–876.

[6] T. J. Lewis and J. Rinzel, *Dynamics of spiking neurons connected by both inhibitory and electrical coupling*, J. Comp. Neurosci. 14 (2003), 283-309.

[7] A. Sherman and J. Rinzel, *Rhythmogenic effects of weak electrotonic coupling in neuronal models*, Proc. Natl. Acad. Sci. USA 89 (1994), 2471–2474.

E-mail address: tim.lewis@nyu.edu